# 14.7 MODELING OF THE EFFECTS OF ACIDIC AEROSOLS ON ARCTIC CLOUD MICROSTRUCTURE AND SURFACE RADIATIVE BUDGET DURING WINTER

Eric Girard, Alexandru Stefanof, Jean-Pierre Blanchet and Rodrigo Munoz-Alpizar
University of Quebec at Montreal, Montreal, Canada

## 1. INTRODUCTION

Wintertime cloud cover over the Arctic ranges between 40 to 50% (Wyser et al., 2008). Low-level mixed phase clouds and optically thin ice tropospheric clouds dominate during the cold season. Grenier et al. (2009) have shown that there are two types of optically thin ice clouds. The first one is characterized by a large concentration of small ice crystals and larger ice crystals in smaller concentration characterize the second one. The latter cloud type is significantly correlated with aerosol concentration. These results suggest that there might be a relationship between the second type of thin ice clouds and large aerosol concentration.

The Arctic remains one of the most polluted regions on Earth during the cold season. High concentrations of aerosols are often observed (Schnell, 1984, Yli-Tuomi et al., 2003). These aerosols are mainly emitted over northern European cities, China, and Siberia. They are transported from the mid-latitudes to the Arctic by the large-scale atmospheric circulation (Barrie et al., 1989, Shaw, 1995). This transport is favored by the southward progression of the polar front during winter. Anthropogenic aerosols are emitted north of the front in an environment with few precipitations, thus limiting the loss of aerosols by wet deposition. Sulphuric acid is an important chemical component of these aerosols and coats most of the aerosols of the accumulation mode (Bigg, 1980).

Laboratory experiments and field observations suggest that acidic coating on ice nuclei can have an important effect on homogeneous and heterogeneous ice nucleation. Archuleta et al. (2005) have shown that the decrease of ice nucleation at temperatures below $-40^0$C by immersion and condensation modes due to sulphuric acid coating is variable and depends on the IN chemical composition. Other laboratory experiments performed at temperatures ranging between –10 and $-40^o$C also show that the heterogeneous freezing temperature initiated by immersion of various mineral dust particles decreases as the percentage by weight of sulphuric acid in the particle increases (Ettner et al., 2004). More recently, Eastwood et al. (2009) have shown that deposition ice nucleation on sulphuric acid-coated kaolinite particles is considerably altered at temperatures below 243K, requiring an additional 30% ice supersaturation for ice nucleation to occur when compared to uncoated particles. Other laboratory experiments on coated and uncoated mineral dust particles have been performed by Knopf and Koop, (2006), Salam et al. (2007) and Möhler et al. (2008). Measurements taken during a field experiment in the Arctic shows that the IN concentration is decreased by 3 to 4 orders of magnitude in Arctic haze events (Borys, 1989).

Blanchet and Girard (1994; 1995) have hypothesized that the ice nucleation inhibition effect of sulphuric acid coating on aerosols can have an important effect on cloud microstructure and on the surface energy budget in the Arctic during winter. According to their hypothesis, the decrease of the ice nuclei concentration leads to the formation of fewer but larger ice crystals. This process leads to the formation of optically thin ice clouds (type 2b) identified by Grenier et al. (2009). Larger ice crystals increase the precipitation rate and the dehydration of the troposphere. The decrease of the ice nuclei concentration can also increase the persistence of mixed-phase clouds in the lower troposphere and favors the formation of larger ice crystals, which precipitate more efficiently. The dehydration of the troposphere initiates a cooling trend at the surface that spreads upward. This results in the decrease of the greenhouse effect due to the strong effect of water vapor, primarily in the broad rotation band. The reduced greenhouse effect further promotes dehydration and cooling cycle (Blanchet and Girard, 1995; Curry et al., 1995). We refer to this process as the dehydration-greenhouse feedback.

In this paper, a review of the main modeling studies on the effect of acidic aerosols on cloud microstructure and surface radiative budget is presented with the addition of the most recent results still unpublished. Each study aims at evaluating the effect of acidic aerosols on cloud microstructure and radiation at the surface. The next section presents results obtained with a column model explicitly simulating the interaction between acidic aerosols and cloud water droplets and ice crystals. The third section is devoted to the simulation of 4 cold seasons using observed aerosol chemical composition and concentration at Alert, Canada. Finally, 3D simulations are presented in section 4 using the Northern Aerosol Regional Climate Model and the limited-area version of the Global Environmental Multiscale (GEM-LAM) model.

**2. Acidic aerosols and mixed-phase clouds at very cold temperatures**

As previously mentioned, the acidic coating on aerosols impacts both on homogeneous and heterogeneous nucleation of ice crystals. In this first modeling study, the impact on homogeneous nucleation is evaluated using an explicit column model.

The microphysics part of the model is based on MAEROS2, an aerosol dynamic model developed by Gelbard et al. (1980). MAEROS2 computes the time evolution of size-segregated particles in the atmosphere including condensed water. Only one phase, liquid or solid, is allowed in a size bin. There are 38 size bins from 0.01 μm to 500 μm. The prognostic variables are the ice and liquid mixing ratios, the aerosol mixing ratio, the specific humidity and the temperature. Deposition and contact ice nucleation are not included in this model. Immersion freezing depends on droplet volume following Bigg formulation (Pruppacher and Klett, 1998). The median freezing temperature of each size bin is calculated using the Bigg equation. When the temperature is below the median freezing temperature, it is assumed that all droplets in a given size bin freeze. The homogeneous freezing temperature of haze droplets is set to -40°C for the non-acidic scenario. In the acidic scenario, the homogeneous freezing temperature depends on the sulphuric acid concentration in the droplets. A detailed description of the radiation and microphysics schemes is given by Girard and Blanchet (2001).
Short simulations (8 days) of the formation of boundary layer clouds in cold environments were performed. Initially, the atmosphere has the properties of a sub-arctic winter maritime air mass. Temperature and humidity advection are neglected. Therefore, the temporal evolution of the temperature depends only on the infrared radiative cooling of the atmosphere with no solar contribution. Time step is less than 1 s.

Figure 1 to 4 shows the liquid/ice water mass and number concentration, the cloud particle mean diameter and the ice supersaturation in the first 3 layers above the ground) as a function of time. During the first 24 hours, the air cools radiatively but remains unsaturated with respect to liquid water. Just before the end of the first day, aerosols are activated and cloud droplets form. At this stage, there are few large droplets as shown by the mean diameter of droplets. As a result, the ice supersaturation remains relatively high with oscillations, which are produced by successive aerosol activations. This process lasts 24 hours during which large ice crystals are nucleated and precipitate out of the liquid layer. This process resumes until the beginning of day 3 when the layer above becomes saturated and cloud forms. At that time, the cooling rate is significantly reduced in the first layer and ice crystals precipitate out of the layer above. As a result, the ice supersaturation in the first layer drops significantly.

The infrared cooling of the atmospheric column resumes and condensate appears in the third layer above the ground at day 5. From day 5 to 8, the source of ice crystals at 970 hPa and 1000 hPa is mainly the sedimentation of ice crystals nucleated aloft. As the ice crystals precipitate, they grow by water vapor deposition and aggregation. This gives rise to the characteristic vertical structure of arctic mixed-phase clouds with a thin layer of liquid at the top of the cloud and larger ice crystals precipitating below. The formation of this type of cloud is possible as long as the homogeneous freezing point of haze droplets is not reached. In the acidic scenario, the homogeneous freezing temperature of haze droplets is much lower compared to the non-acidic scenario. Therefore, clouds can remain in mixed-phase a longer period of time at colder temperatures. In the non-acidic case, when the

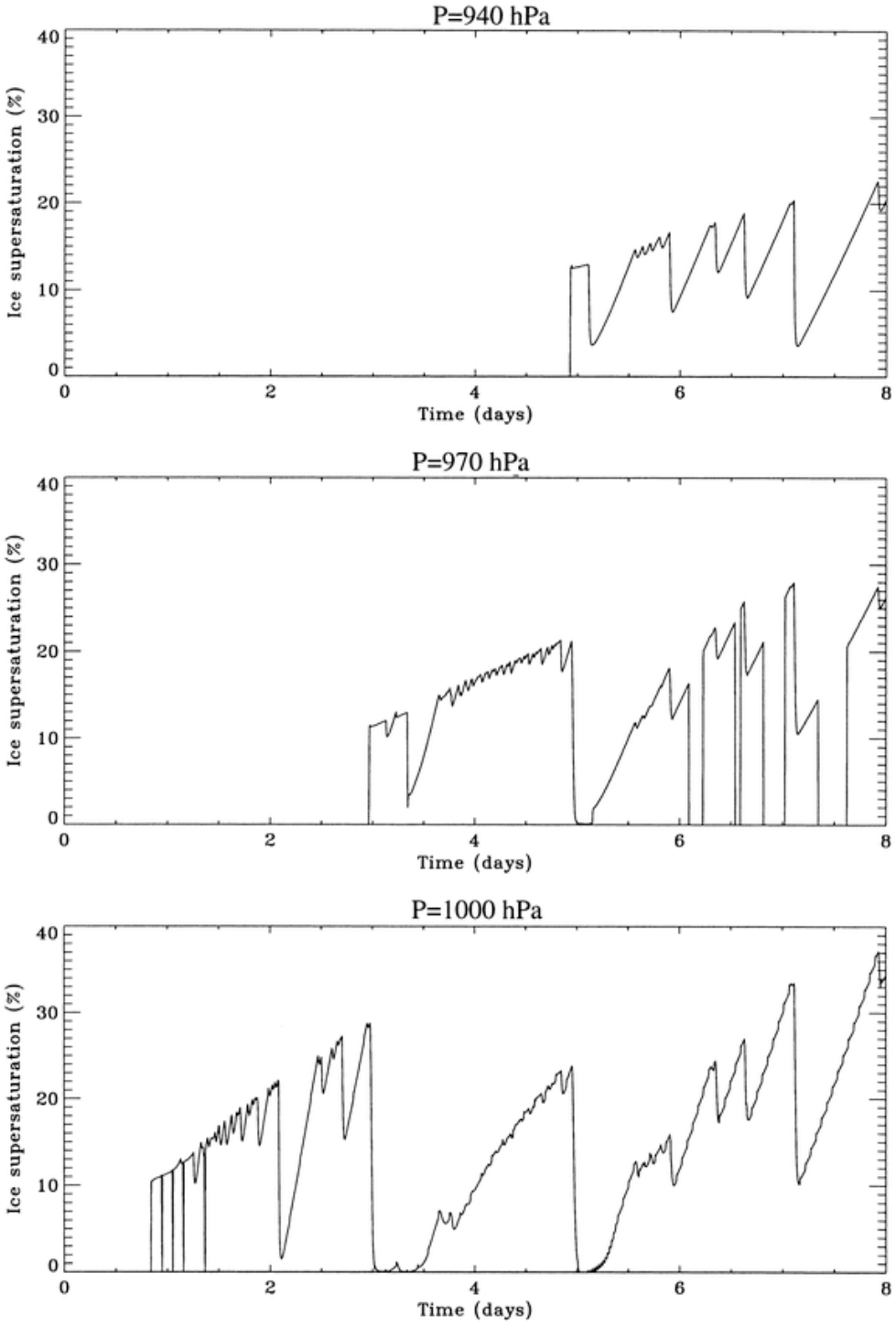


Figure 1: Ice supersaturation time evolution at 1000 hPa, 970 hpa and 940 hPa (after Girard and Blanchet, 2001).

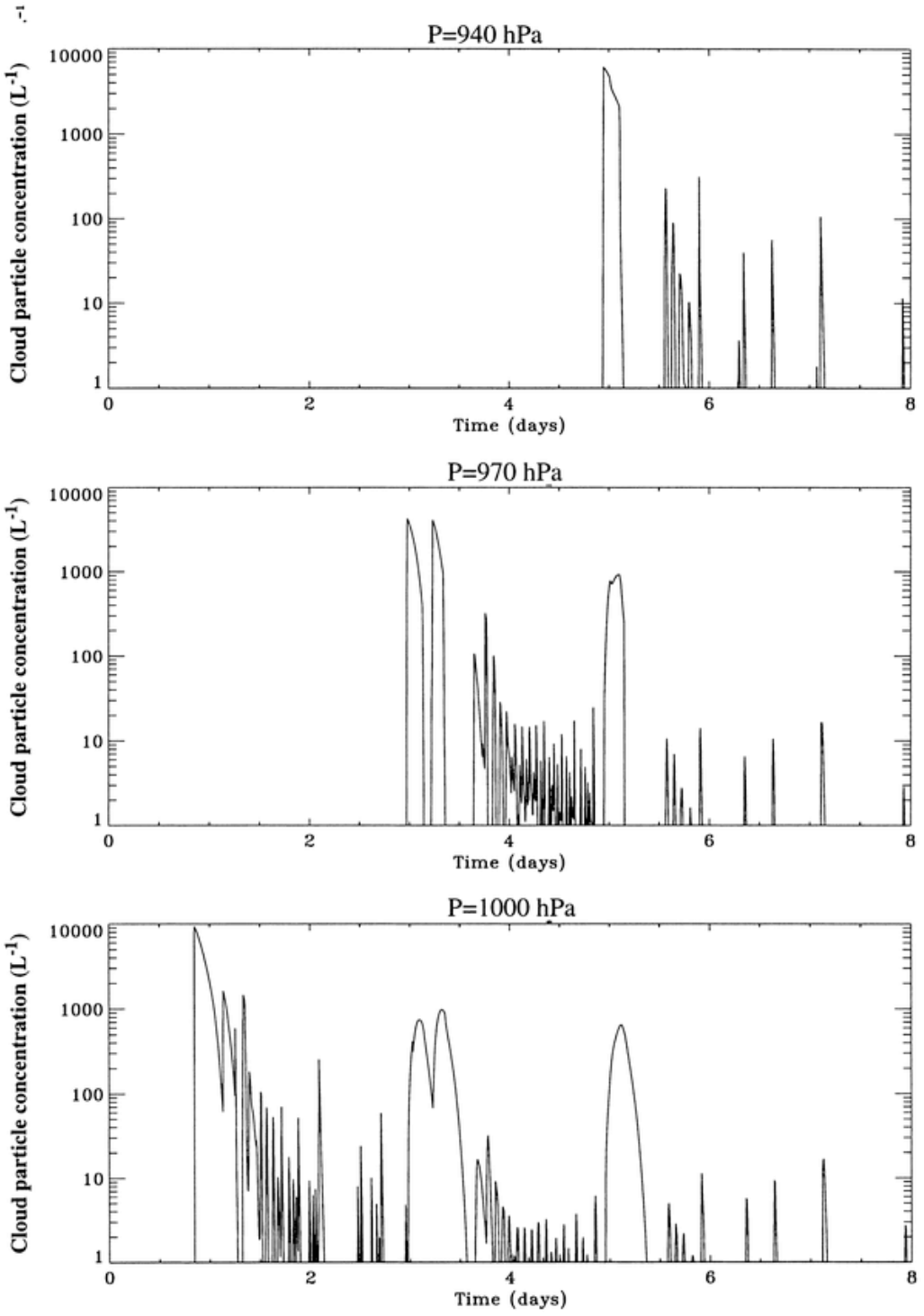


Figure 2 : Cloud particle concentration vs time at 1000 hPa, 970 hpa and 940 hPa (after Girard and Blanchet, 2001).

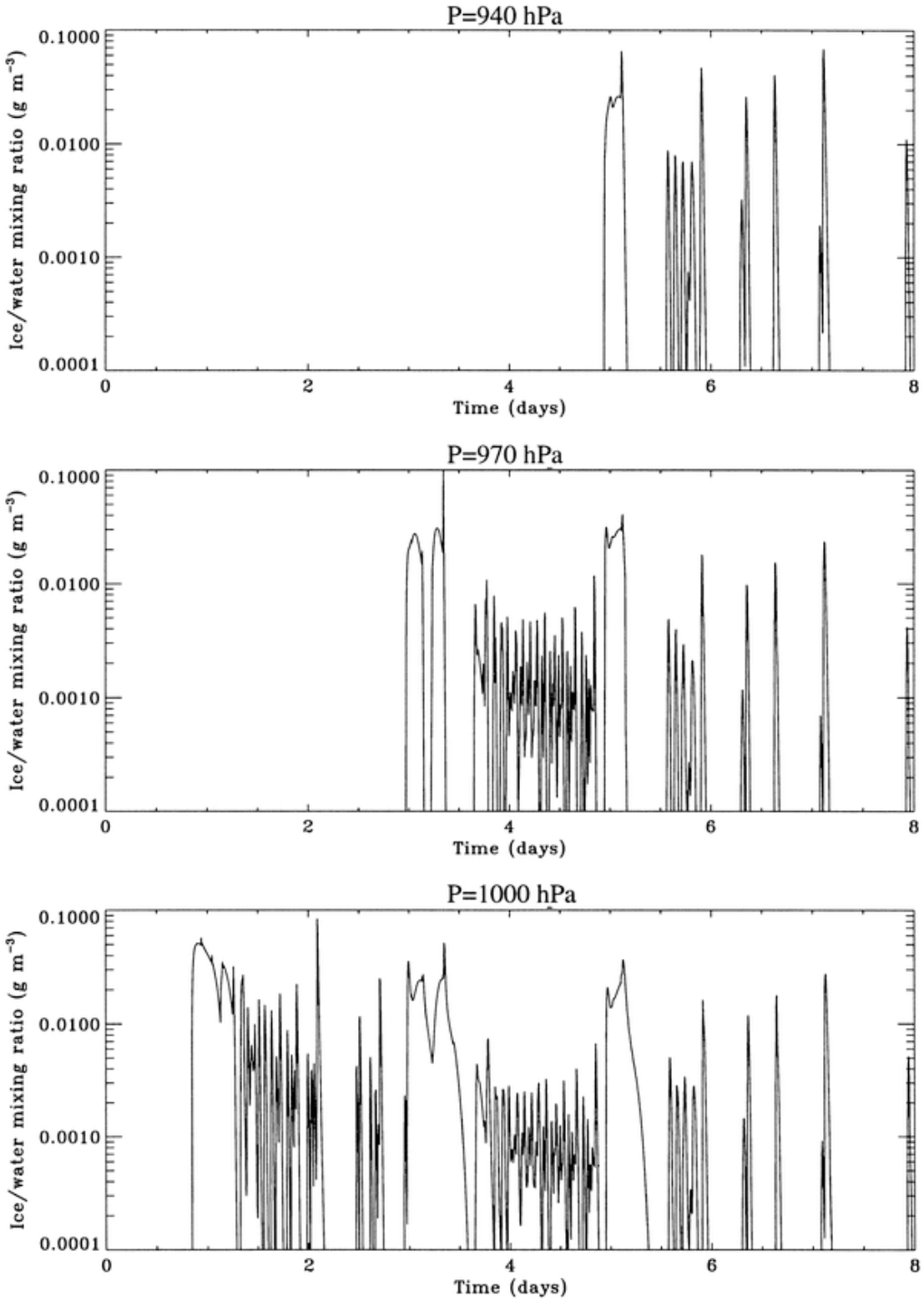


Figure 3: Ice/water mixing ratio vs time at 1000 hPa, 970 hpa and 940 hPa (after Girard and Blanchet, 2001).

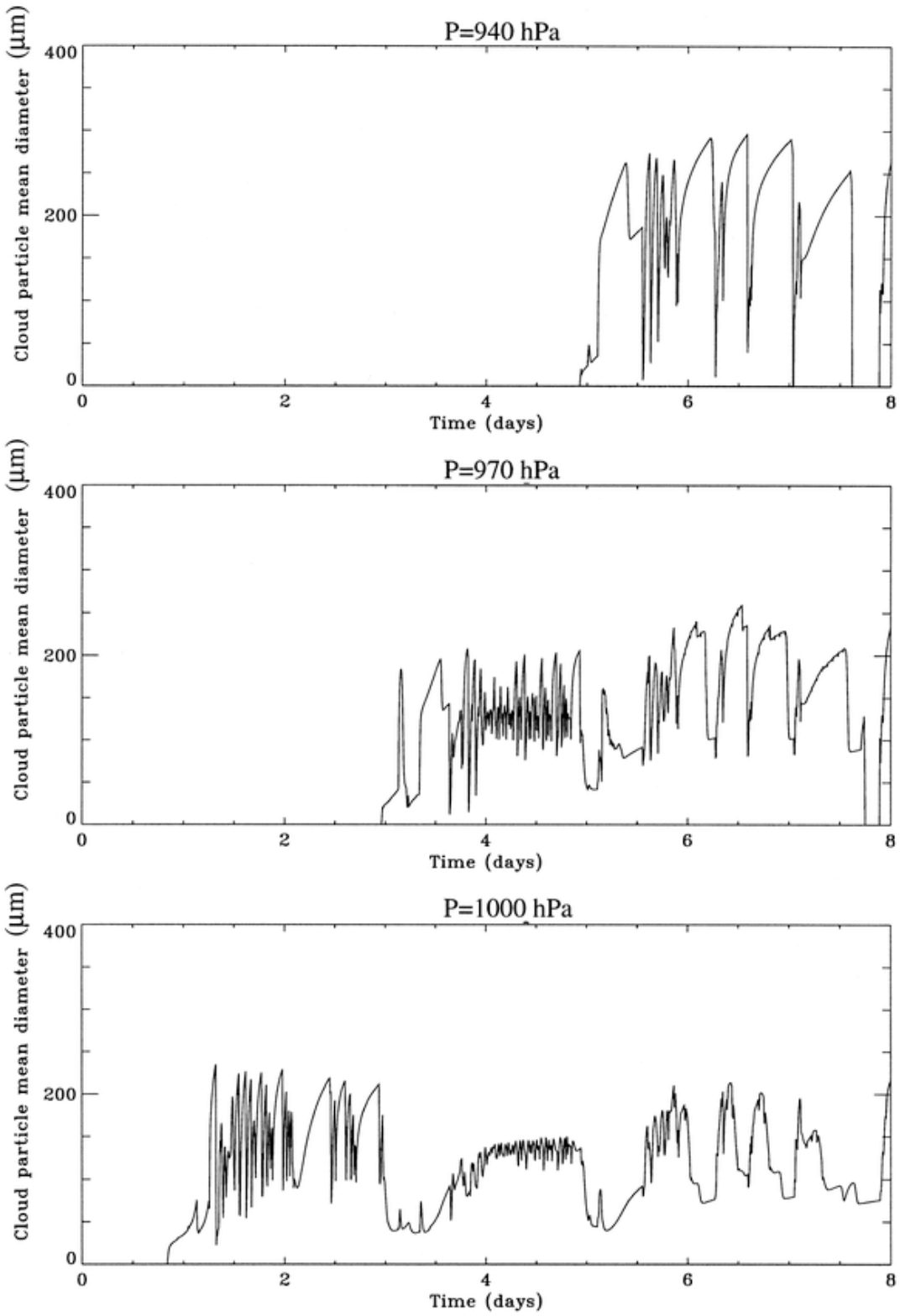


Figure 4: Cloud particle mean diameter vs time at 1000 hPa, 970 hpa and 940 hPa (after Girard and Blanchet, 2001).

homogeneous freezing temperature is reached, haze droplets freeze and act as ice nuclei. The largest aerosols are then activated and a large number of small ice crystals are nucleated. Ice supersaturation decreases rapidly to near 0. It is the formation of an ice fog.

This relatively simple modeling experiment shows that acidic aerosols can have an effect on cloud formation at cold temperatures. However, several approximations were made. The heterogeneous freezing of cloud droplets includes only the immersion mode. Eastwood et al. (2009) have shown that aerosols coated with sulphuric acid can also modify the ice nucleation by deposition, which is not considered in this experiment. Furthermore, the contact nucleation is also neglected. The model configuration (the fact that water droplets and ice crystals cannot co-exist in the same size bin) does not allow to account for these freezing processes. Finally, this model cannot be used for long simulations due to computational cost.

**3. Simulation of four cold seasons at Alert**

In order to perform longer simulations and include all freezing modes, the single-column version of the Canadian General Circulation Model is used coupled with the Canadian Aerosol Module to simulate the aerosol size distribution explicitly (Gong et al., 2003). This model includes the 2-moment microphysics scheme of Girard and Curry (2001). In this model, acidic aerosols have also an impact on heterogeneous ice nucleation in addition to the effect on homogeneous freezing of haze droplets.

Simulations of four cold seasons (from November to May) were performed over Alert (Canada) for the period 1991 to 1994. Aerosol observations near the surface were available at this arctic research station for this period and used for our simulations together with 12-hour aerological soundings. These observations were used to calculate the dynamical tendencies with the residual iterative method (Girard and Blanchet 2001). Three aerosol scenarios were considered for our simulations: (1) a natural aerosol case; (2) an acidic scenario that distinguishes form the latter by fewer ice nuclei concentration and lower homogeneous freezing temperature of haze particles. In this scenario, the decrease of ice nuclei and the amount to which the homogeneous freezing temperature of haze particles is reduced is a function of the observed aerosol acidity (see section 4, equation 1); and (3) a very acidic scenario in which the decrease of ice nuclei and homogeneous freezing temperature is always applied whatever the aerosol composition.

Results show that the total water averaged over the four cold seasons (total water includes water vapor, liquid and ice water) decreases substantially in the two acidic cases below 500 hPa (see Figure 5). Due to the decrease of ice nuclei concentration, fewer ice crystals are nucleated (not shown). This leads to the formation of ice crystals with a larger diameter since the water vapor available to deposit on each ice crystal increases. Therefore, ice crystals are more efficient to precipitate and dehydrate the lower atmosphere. Figure 5 shows that the temperature vertical profile is modified in acidic scenarios with colder temperature near the surface and in the lower troposphere, thus reducing the greenhouse effect locally. This effect gradually decreases as we go upward in the atmosphere. Girard et al. (2005) have shown that the effect of acidic aerosols on the surface radiative budget is maximum in February and March, which coincides with the coldest part of the year combined with the peak of sulphuric acid concentration.

An analysis of aerosol and weather observations, which were taken during the same years at Alert, have shown that acidic aerosols favor low-level ice crystals precipitating to the surface, a common phenomenon in the Arctic during winter (Curry et al., 1990). However, the time and spatial resolution of the aerosol dataset (aerosols were measured only once a week near the surface) were not high enough to unravel this potential link between acidic aerosols and precipitating ice crystals.

**4. Pan-Arctic 3D simulations**

A natural extension to the investigation of Girard et al. (2005) consists in assessing the magnitude of the cooling effect of acidic aerosols over the whole Arctic basin and the impact of the Arctic

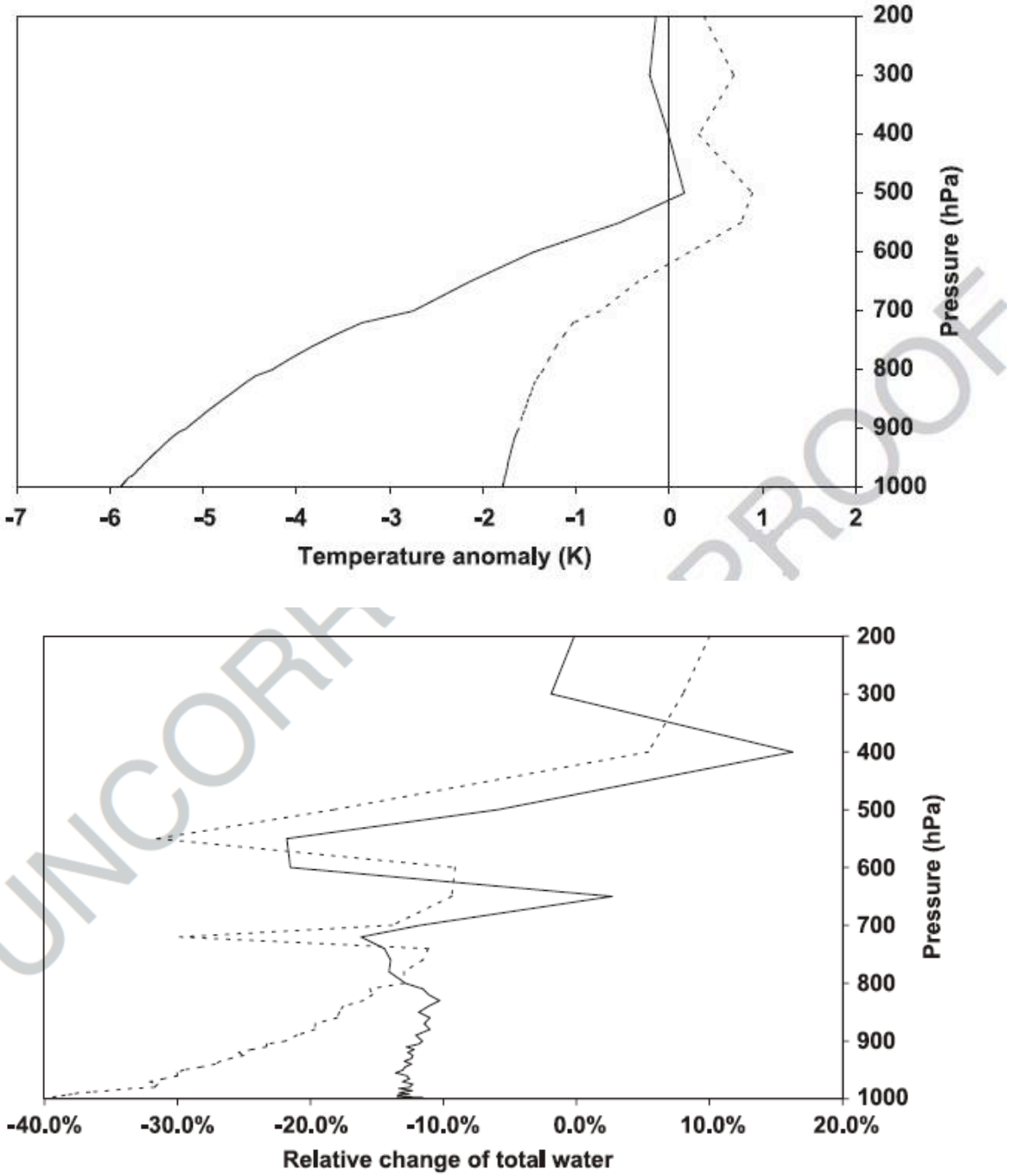


Figure 5: Temperature and total water anomalies averaged over the 4 cold seasons at Alert for the very acidic scenario (dotted line) and the acidic scenario (full line) (after Girard et al., 2005).

cooling on the large-scale atmospheric circulation. Two limited-area models were used to perform the simulations: the Northern Aerosol Regional Climate Model (Gong et al., 2003) and the Global Environmental Multiscale Model (Côté et al., 1998). The months simulated include February 1990, December to February 1997-1998 and January and February 2007.

### 4.1 NARCM simulations

The Northern Arctic Regional Climate Model (NARCM) is a limited-area non-hydrostatic climate model with a dynamic size-distributed aerosol scheme. The numerical formulation of NARCM is derived from the Canadian Regional Climate Model (Caya and Laprise, 1999). It is based on the fully elastic, non-hydrostatic Euler field equations solved with a state-of-the-art semi-implicit and semi-Lagrangian (SISL) marching algorithms adequate for computing atmospheric flow at all spatial scales. CRCM atmospheric variables are discretized on an Arakawa C-type staggered grid on a polar-stereographic projection in the horizontal and Gal-Chen terrain-following scaled height coordinate in the vertical (Gal-Chen and Somerville, 1975). NARCM simulates aerosol explicitly with 12 size bins from 0.005 to 20.48 μm (Gong *et al*., 2003). The aerosol module CAM is a size-segregated multi-component algorithm that treats five major types of aerosols: sea-salt, sulphate, black carbon, organic carbon and soil dust. It includes major aerosol processes in the atmosphere: production, growth, coagulation, nucleation, condensation, dry deposition, below-cloud scavenging, activation, a cloud module with explicit microphysical processes to treat aerosol-cloud interactions, and chemical transformation of sulphur species in clear air and in clouds. Each of these aerosol processes is strongly dependent on particle size, thus requiring an explicit representation of the size distribution.

The parameterizations of physical processes are from the Canadian GCM (McFarlane et al., 1992). The microphysics scheme is from Lohmann and Roeckner (1996). Contact and immersion freezing are parameterizaed following Levkov et al. (1992). Deposition nucleation is not included in this scheme. The microphysics scheme has been modified to include the effect of acidic aerosols on cloud ice nucleation. Two scenarios are considered: the natural aerosol scenario (hereafter scenario A) in which sulphuric acid has no effect whatsoever on the ice nucleation and the acidic scenario (hereafter scenario B), the ice nuclei concentration is decreased when sulphate aerosol concentration reaches values above the monthly mean concentration of sulphate over the domain. The decrease of ice nuclei concentration is based on Borys (1989) observation and is given by an exponential function, which depends on sulphate concentration following Girard et al. (2005) as follows:

$$Fr = 10^{-[B * m(SO_4)]} \quad (1)$$

where $Fr$ is the IN reduction factor, $m(SO_4)$ is the sulphate concentration and $B$ is a constant chosen so that $Fr$ = 0.001 when the maximum sulphate concentration during the simulation is reached. In scenario B, $Fr$ is multiplied by the IN concentration. Both immersion and contact nuclei are reduced in the experiment.

The simulation domain covers most of Europe, Northern Canada, Siberia and the Arctic. The month of February 1990 is simulated. Initial and boundary conditions are provided by the NCEP analyses. Sulphate emissions are provided by datasets of Bates et al. (1992) for DMS and by Kettle et al. (1999) for H2S. Anthropogenic sources of sulphate are from Benkovitz et al. (1996). An ensemble of 12 simulations is performed for each scenario. Each simulation within an ensemble is initialized with different initial conditions following Rinke and Dethloff (2000). Results presented below always represent the ensemble mean of either aerosol scenario A or B and shadowed areas indicate that results are statistically significant with a confidence level of 95%.

Figure 6 shows the monthly mean sulphate vertical path difference between scenario B and A. The sulphate vertical path is much larger in scenario B with spatially averaged difference of 44%. These differences are discussed at the end of the section. In both scenarios, there is a ridge of sulphate concentration stretching from Siberia to the Canadian Arctic. This pattern is typical of the sulphate concentration in the Arctic during winter (Barrie et al., 1989). Sulphate emitted over the industrial areas of Eurasia are transported by the dominant winds induced by the persistent low pressure system east of Greenland and the high pressure system over Siberia.

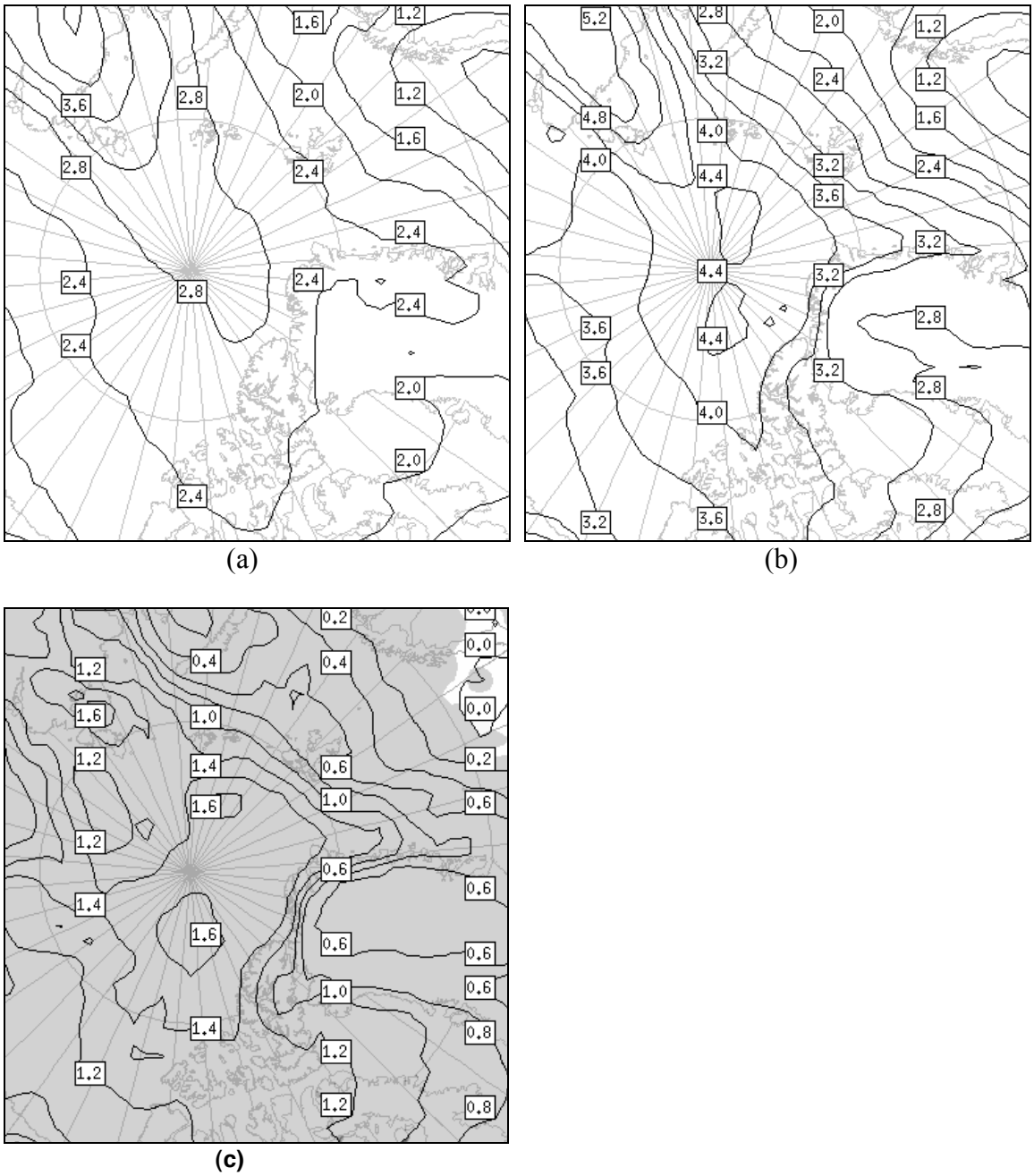


Figure 6: February mean sulphate vertical path for (a) aerosol scenario A, (b) aerosol scenario B, and (c) scenario B minus scenario A (units are kg $m^{-2}$) (after Girard and Stefanof, 2007).

Figure 7 shows the liquid and ice water path difference between scenario B and A. As expected, the ice water path decreases the most over cold areas and where the sulphate vertical path is the largest. Over Northern Europe, sulphate concentrations are large but temperature is relatively warm. At warm temperatures, the ice nuclei (IN) concentration is low. As a result, reducing the IN concentration in scenario B over these regions leads to IN concentration approaching 0 $L^{-1}$. This is why the liquid water path substantially increases over warmer regions. Over cold areas of the Arctic, the same IN decrease does not have the same

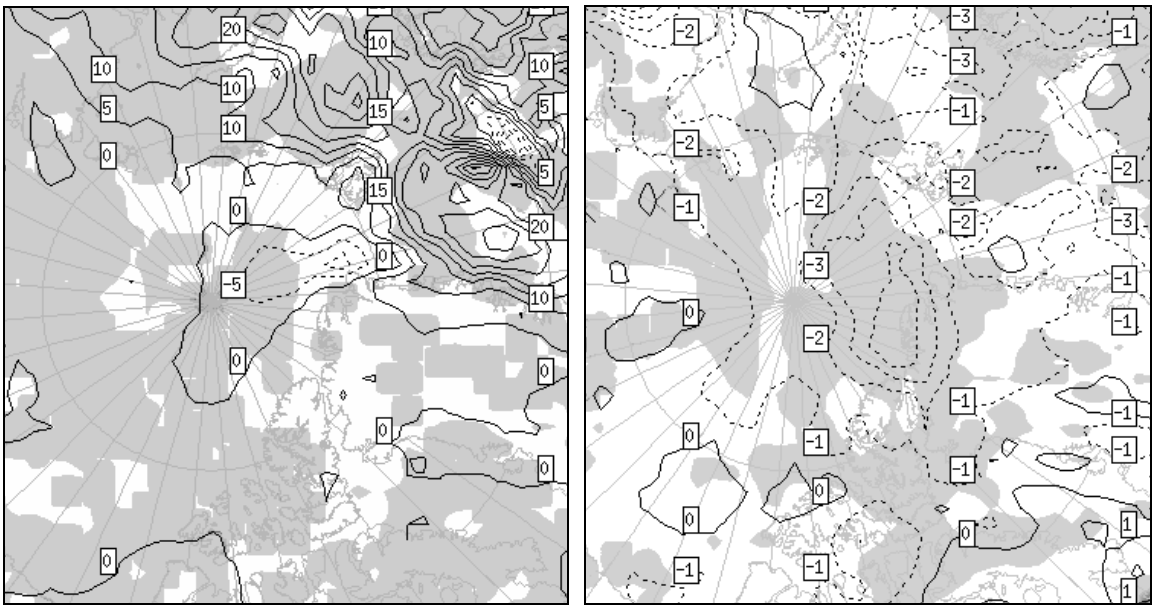


Figure 7: February mean difference between aerosol scenarios B and A for (a) liquid water path (kg $m^{-2}$) and (b) ice water path (kg $m^{-2}$) (after Girard and Stefanof, 2007).

effect due to the fact that the IN concentration is much larger at these temperatures. Even with the IN reduction in scenario B, the IN concentration is still well above 0 $L^{-1}$. The reduced concentration of ice crystals favors a faster growth of each ice crystal by the Bergeron process. Figure 8 shows that this leads to an increase of the monthly mean precipitation rate over the coldest regions.

The increased precipitation rate in scenario B contributes to enhance the dehydration of the troposphere. The total water (condensate and water vapor; figure not shown) is reduced. Since water vapor is by far the most efficient greenhouse gas in the atmosphere, this process leads to a decrease of the greenhouse effect over the coldest regions of the Arctic. Figure 8 shows that the monthly mean downwelling infrared radiation at the surface is significantly reduced by up to 12 W $m^{-2}$. As expected, the temperature anomalies are negative with values up to -3 K (see Figure 9**).** Figure 9 shows that the temperature anomaly is the largest at the surface and decreases with height.

In aerosol scenario B, colder temperature over the Arctic combined with warmer tropospheric temperature over Northern Europe and Siberia strengthens the baroclinic zone, particularly over Northern Europe and the Laptev Sea. As a result, the monthly mean wind velocity increases by up to 3 m s-1 over the Laptev Sea at 500 hPa (see Figure 10). The increased sulphate concentration over the Arctic in scenario B (see Figure 6) is explained by the wind strengthening in the baroclinic zone over Northern Europe.

This investigation has shown that the results obtained with the single-column model at Alert (see previous section) are not confined over a small region but rather over a large area covering the coldest part of the Arctic. This investigation has also shown that the initial cooling of the Arctic produced by the interaction between acidic aerosol and clouds positively feedbacks on the general circulation allowing to increase even more the aerosol concentration and the effect of acidic aerosols. Other months (December to February 1997-1998) have also been simulated and the results are very similar to February 1990 (Munoz-Alpizar et al., 2009).

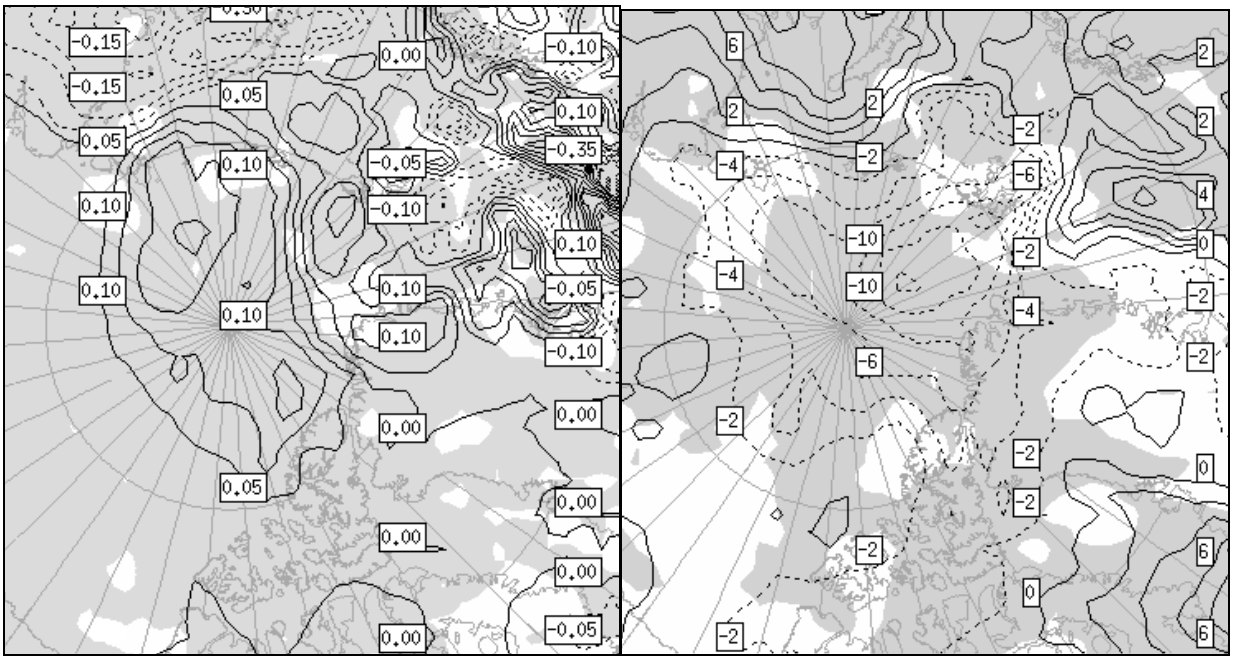

Figure 8: February mean difference between aerosol scenarios B and A for precipitation (mm/day) (left panel) and downwelling infrared radiation flux at the surface (W $m^{-2}$) (right panel) (after Girard and Stefanof, 2007).

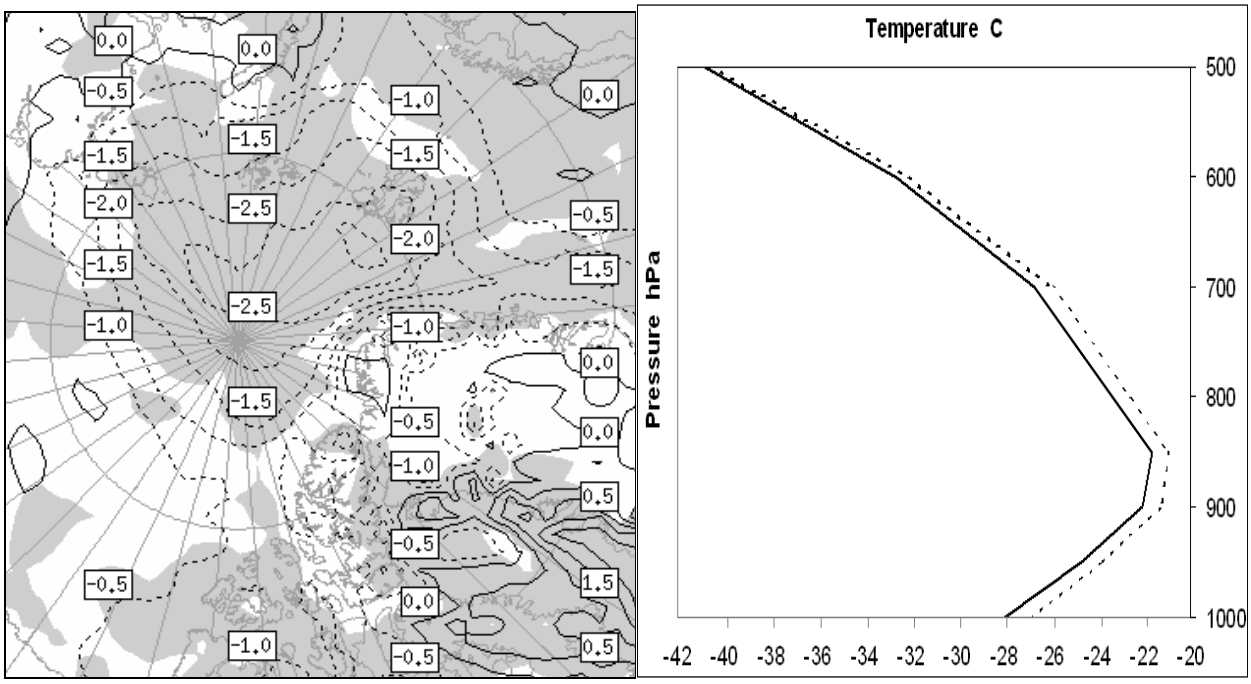


Figure 9: February mean difference between aerosol scenarios B and A for (a) surface air temperature (K) over the domain and (b) mean vertical profile of temperature averaged over grid points with sea ice cover (full line for aerosol scenario B and dotted line for aerosol scenario A) (after Girard and Stefanof, 2007).

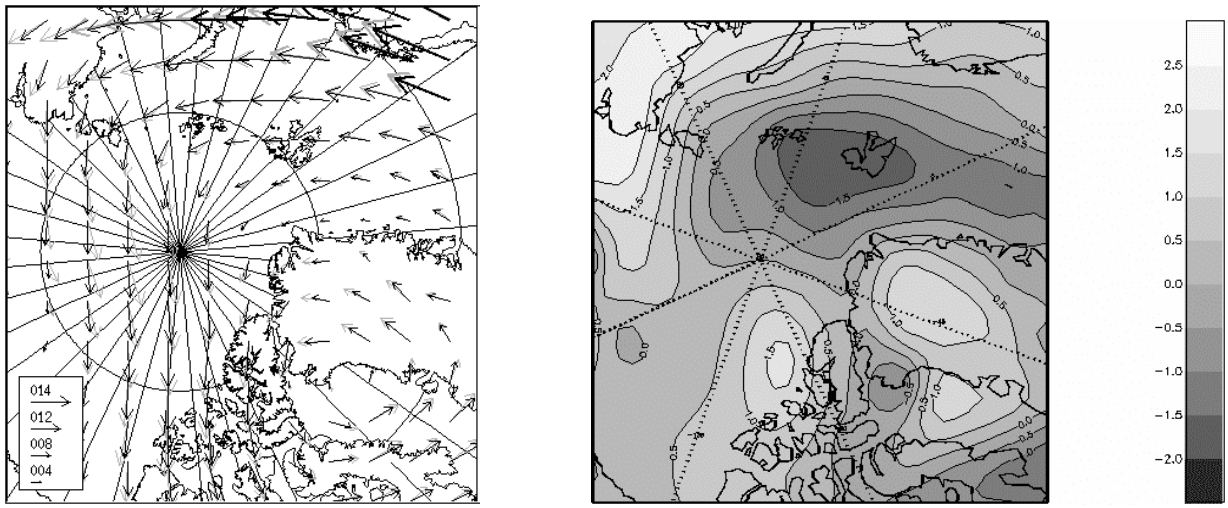

Figure 10: February mean difference between aerosol scenarios B and A for 500 hPa wind (a) direction (black arrows for scenario A and grey arrows for scenario B) and (b) velocity (knots) (after Girard and Stefanof, 2007).

**4.2 GEM-LAM simulations**

The modeling experiments presented in previous sections have shown that the alteration of acidic aerosols on ice nucleation can have an important effect on the surface radiative budget over the Arctic during winter. However, in these modeling studies, the acidic aerosol scenario was treated rather subjectively. Indeed, the decrease of ice nuclei concentration was a function of the sulphate concentration using an exponential function and was based on Borys (1989) observations of IN decrease in polluted events. The choice of an exponential function was subjective. Furthermore, it was assume that all ice nucleation modes (both deposition and freezing modes) were altered equally by the presence of sulphuric acid.

In this new modeling study, the objective is to refine the representation of the IN decrease due to acidic coating to get a more realistic evaluation of the potential effect of anthropogenic aerosols on arctic wintertime cloud and surface radiative budget. Laboratory data from Eastwood et al. (2009) on ice nucleation on uncoated and sulphuric acid-coated kaolinite particles are used to develop a more physically-based parameterization of deposition ice nucleation.

The Global Environmental Multiscale (GEM) Model is used for this study. A detailed description of this model is given by Côté et al. (1998). GEM does not simulate aerosol emission and transport. Therefore, aerosols chemical composition is prescribed in our simulations. The microphysics scheme is from Kong and Yau (XXXX). This scheme predicts the liquid and ice mixing ratios and includes the ice crystal sedimentation. The parameterization of ice nucleation has been modified for our experiments. The parameterization of contact ice nucleation is from Lohman and Diehl (2006) and immersion freezing is from Lohman and Roekner (1996). The parameterization of deposition ice nucleation is based on laboratory experiment of Eastwood et al. (2009) on kaolinite (uncoated and sulphuric acid coated) particles. The parameterization is based on the classical theory of ice nucleation in which the contact angle ($\Theta$) between the ice embryo and the particle is parameterized as a function of temperature as follow:

$$\Theta = aT + b \qquad (2)$$

where a and b are constant and have distinct values for uncoated and sulphuric-acid coated kaolinite particle. Eastwood et al. (2009) have shown that the effect of sulphuric acid coating on deposition ice nucleation on kaolinite particles is the largest below -30$^0$C.

The simulation domain is centered over the Arctic and covers the region north of 50N. The month of January and February 2007 are simulated. Initial and boundary conditions are provided by the ECMWF re-analyses. The horizontal resolution is

$0.25^0$ with 53 levels in the vertical. Two aerosol scenarios are considered: Scenario A in which it is assumed that ice nuclei are uncoated and scenario B in which ice nuclei are coated with sulphuric acid. The appropriate equation for the contact angle is chosen according to the scenario. An ensemble of 10 simulations is performed for each scenario. Each simulation within an ensemble is initialized with different initial conditions. Results presented below always represent the ensemble mean of either aerosol scenario A or B and shadowed areas indicate that results are statistically significant with a confidence level of 95%.

Figure 11 shows the temperature difference between scenario B and A for January and February 2007 at 1000 hPa, 850 hPa and 500 hPa. Results are consistent with the previous modeling studies with a cooling over the Arctic that spreads throughout the troposphere. A cooling of up to 3K, 1K and 0.8K is obtained over the Central Arctic at the surface, 850 hPa and 500 hPa respectively. This cooling is associated to statistically significant decrease of the water vapor path over much of the Arctic in scenario B (see Figure 12a) and a decrease of the downwelling infrared radiation at the surface up to -12 W $m^{-2}$ (not shown).

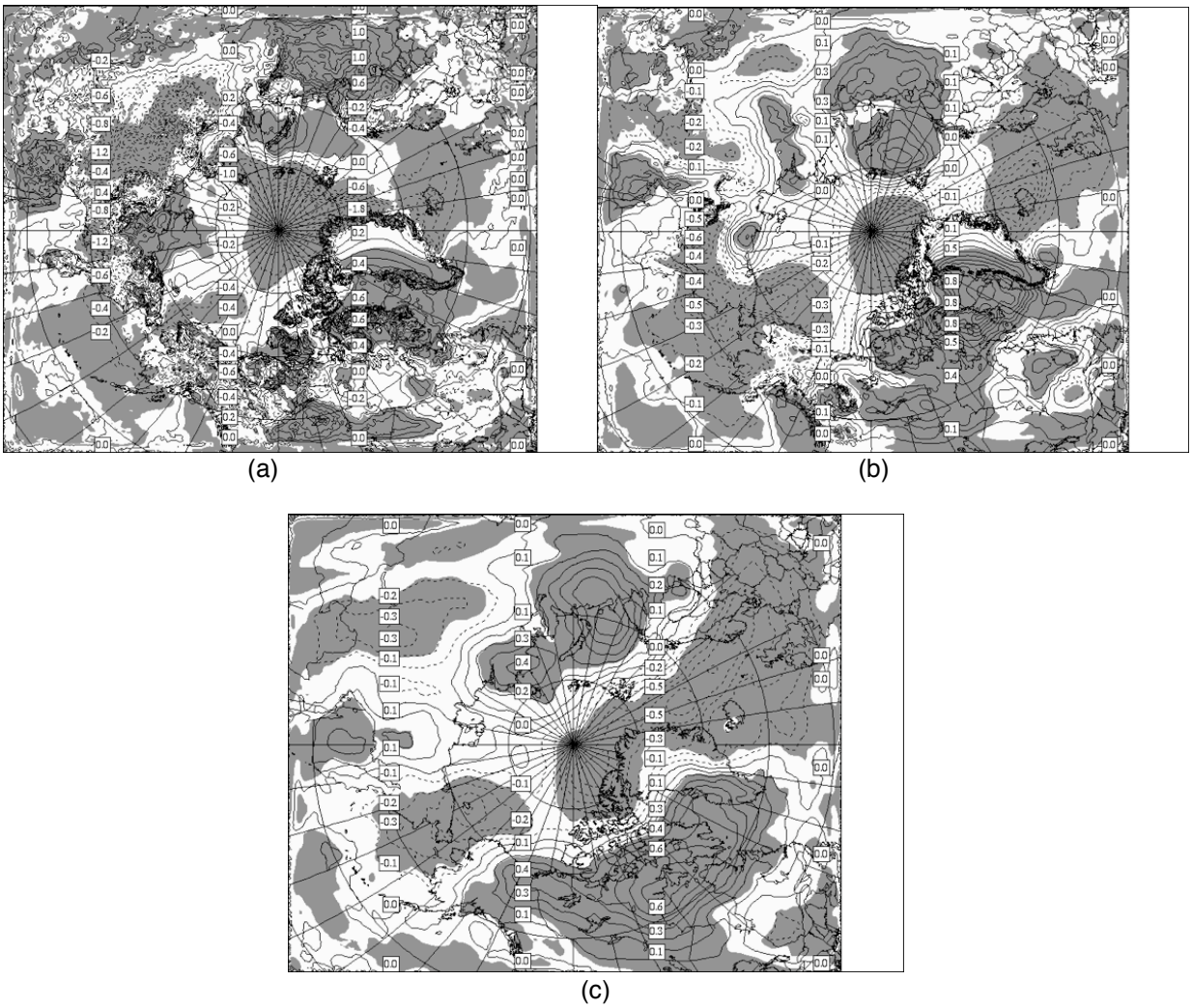

(a) (b)

(c)

Figure 11 : : January/February mean difference between aerosol scenarios B and A for (a) surface air temperature (K), (b) 850 hPa temperature and (c) 500 hPa temperature over the domain.

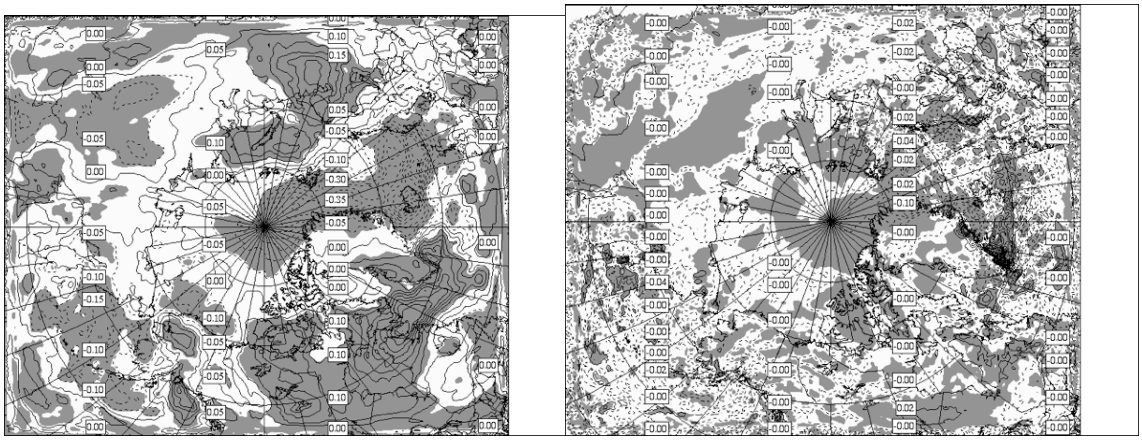

Figure 12 : January/February mean difference between aerosol scenarios B and A for (a) water vapor path and (b) precipitation (accumulated over 3h) over the domain.

Figure 12b show the precipitation accumulation (over 3 hours) difference between scenario B and A. There is a decrease of precipitation in scenario B over a large part of the Arctic. Although this difference is small, it is statistically significant. The decrease of precipitation is not consistent with the atmospheric cooling. To ensure that this decrease of precipitation is not caused by large precipitation events (not representative of the whole month), the precipitation rate is plotted as a function of the water vapor path for the area covering the surface cooling over the Arctic (see Figure 14). The water vapor path is a good indicator of the atmospheric temperature. Figure 13 shows that the precipitation rate is larger in scenario B at cold temperature. At warmer temperature, the precipitation rate is smaller when compared to scenario A. In the latter scenario, a few large precipitation events occur at the warmest temperatures (or highest water vapor path). These events are likely to be associated to the passage of low-pressure systems that brings milder and moist air over the Arctic. At colder temperatures, scenario B produces more precipitation, which is consistent with the cooling obtained over this area. Note the higher concentration of points at colder temperature (or lower water vapor path values). This indicates that the mean precipitation value for scenario A is biased by few precipitation events at warm temperatures and is not representative of the whole period.

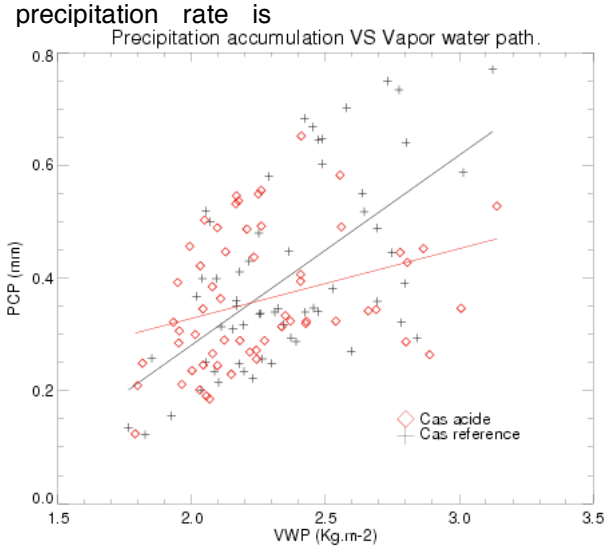


Figure 13: Daily precipitation accumulation for January and February as a function of the daily mean water vapor path over the negative surface air temperature anomaly in the Arctic. Red line represents aerosol scenario B and black line represents aerosol scenario A.

## 5. Summary and Conclusion

Previous field and laboratory experiments have shown that acidic aerosols may significantly decrease the ability of aerosols to nucleate ice crystals. In this research, we evaluate the effect of decreasing the IN concentration on cloud formation and radiative budget of the Arctic for a month of February. The Arctic is characterized by episodes of high acidic concentration during winter (known as Arctic haze). Blanchet and Girard (1994) have hypothesized that, through their ability to reduce IN concentration, acidic aerosols can affect cloud microphysics and increase precipitation originating from boundary layer mixed-phase clouds. Enhanced precipitation dehydrates the troposphere, thus reducing the greenhouse effect. As a result, the surface air temperature decreases. If this process occurs over a long period of time, it could lead to a surface cooling detectable on monthly time scale. This process is known as the dehydration-greenhouse feedback (DGF).

Simulations using a detailed size-bin aerosol-cloud single-column model have shown that the decrease of the homogeneous freezing temperature of acidic haze droplets favors the formation of fewer but larger ice crystals. The DGF was later evaluated over a single location (Alert) for 4 cold seasons by Girard et al. (2005). Results have shown that the DGF produces a substantial cooling in the lower troposphere. In this research, we extend the previous study to the whole Arctic for a month of January and February, which are the months during which the DGF surface cooling was the largest in the Girard et al. (2005) investigation.

The effect of acidic aerosols on clouds and surface radiative budget over the Arctic has also been evaluated over the whole Arctic for winter months with two 3D models. The first 3D investigation with the NARCM model for February 1990 have shown that the DGF can cool the lower troposphere by as much as 3K over the Central Arctic. Simulation of January and February 2007 with the GEM model (including a new ice nucleation parameterization on uncoated and sulphuric acid-coated ice nuclei based on recent laboratory experiments) have shown similar results. The GEM simulation results combined with the previous modelling studies discussed in this paper have shown that the DGF could be important during winter.

Recent analysis of the CloudSat and Calipso images for midwinter 2007 by Grenier et al. (2009) suggest a link between aerosol and clouds composed of large ice crystals (optically thin ice clouds). Modeling experiments presented in this paper and laboratory experiment of ice nucleation on sulphuric-coated and uncoated mineral particles support the idea that clouds observed by satellites (Grenier et al., 2009) may be related to acidic aerosols. However, in-situ measurements will be necessary to confirm this hypothesis.

## 6. Acknowledgements

The authors would like to thank the Canadian Foundation for Climate and Atmospheric Sciences (CFCAS), the National Sciences and Engineering Research Council of Canada (NSERC) and the Fonds québécois de la recherche sur la nature et les technologies (FQRNT) for their funding support.

## 7. References

Archuleta, C.M., DeMott, P.J., Kreidenweis, S.M. 2005. Ice nucleation by surrogates for atmospheric mineral dust and mineral dust/sulfate particles at cirrus temperatures. *Atmospheric Chemistry and Physics* **5:** 2617-2634.

Barrie, L.A., Olson M.P., Oikawa, K.K. 1989. The flux of anthropogenic sulphur into the Arctic from mid-latitudes. *Atmospheric Environment* **23:** 2502-2512.

Bates, T.S., Lamb, B. K., Guenther, A., Dignon, J., Stoiber, R.E. 1992. Sulfur Emission to the Atmosphere from Natural Sources. *Journal of Atmospheric Chemistry* **14:** 315-337.

Benkovitz, C.M., Scholtz, M.T., Pacyna, J., Tarrason, L., Dignon, J., Voldner, E.C., Logan, P.A., Graedel, T.E. 1996. Global gridded inventories of anthropogenic

emissions of sulphur and nitrogen. *Journal of Geophysical Research* **101:** 29 239-29 253.

Bigg, E.K., 1980. Comparison of aerosol at four baseline atmospheric monitoring stations. *Journal of Applied Meteorology* **19:** 521-533.

Blanchet, J.-P., Girard, E. 1994. Arctic greenhouse cooling. *Nature* **371:** 383.

Blanchet, J.-P., Girard, E. 1995. Water-vapor temperature feedback in the formation of continental Arctic air: Implications for climate. *Science of the Total Environment* **160/161:** 793-802.

Caya, D., Laprise, R. 1999. A Semi-Implicit Semi-Lagrangian Regional Climate Model: The Canadian RCM, *Monthly Weather Review* **127:** 341-362.

Curry, J.A., Schramm, J.L., Serreze, M.C., Ebert, E.E. 1995. Water vapor feedback over the Arctic Ocean. *Journal of Geophysical Research* **100:** 14 223-14 229.

Eastwood, M. L., S. Cremel, M. Wheeler, B. J. Murray, E. Girard, A. K. Bertram, 2009. Effects of sulphuric acid and ammonium sulphate coatings on the ice nucleation properties of kaolinite particles. *Geophysical Research Letter*, **36**, doi:10.1029/2008GL035997

Ettner, M., Mitra, S.K., Borrmann, S. 2004. Heterogeneous freezing of single sulfuric acid solution droplets: laboratory experiments utilizing an acoustic levitator. *Atmospheric Chemistry and Physics* **4:** 1925-1932.

Gal-Chen, T., Somerville, R. C. 1975. On the Use of a Coordinate Transformation for the Solution of Navier-Stockes. *Journal of Computational Physics* **17:** 209-228.

Gelbard, F.Y., Y. Tambour, J.H. Seinfeld, 1980. Sectional representation for simulating aerosol dynamics. J. Colloid Interface Sc., **76**, 541-556.

Girard, E., Blanchet, J.-P. 2001a. Simulation of Arctic diamond dust and ice fog and thin stratus using an explicit aerosol-cloud-radiation model. *Journal of Atmospheric Sciences* **58:** 1199-1221.

Girard, E., Blanchet, J.-P. 2001b. Microphysical parameterization of Arctic diamond dust, ice fog and thin stratus for climate models. *Journal of Atmospheric Sciences* **58:** 1181-1198.

Girard, E., Blanchet, J.-P., Dubois, Y. 2005. Effects of sulphuric acid aerosols on wintertime low-level atmospheric ice crystals, humidity, and temperature at Alert, Nunavut. *Atmospheric Research* **73:** 131-148.

Girard, E., A. Stefanof, 2007. Assessment of the dehydration-greenhouse feedback over the Arctic during February 1990. *International Journal of Climatology*, **27**: 1047-1058.

Gong, S.L., Barrie, L.A., Blanchet, J.-P., Salzen, K.v., Lohmann, U., Lesins, G., Spacek, L., Zhang, L.M., Girard, E., Lin, H., Leaitch, R., Leighton, H., Chylek, P., Huang, P. 2003. CAM: A Size Segregated Simulation of Atmospheric Aerosol Processes for Climate and Air Quality Models 1. Module Development, *Journal of Geophysical Research* **108:** D1**.**

Grenier, P., J.-P. Blanchet, R. Munoz-Alpizar, 2009. Study of polar thin ice clouds and aerosols seen by CloudSat and Calipso during midwinter 2007. *Journal of Geophysical Research*, **114**, doi:10.1029/2008JD010927

Kettle, A. J., Andreae, M. O., Amouroux, D., Andreae, T. W., Bates, T. S., Berresheim, H., Bingermer, H., Bonforti, R., Curran, M.A.J., diTullio, G.R., Helas, G., Jones, G.B., Keller, M.D., Kiene, R.P., Leck, C., Levasseur, M., Malin, G., Maspero, M., Matrai, P., McTagart, A.R., Mihalopoulos, N., Nguyen, B.C., Novo, A., Putaud, J.P., Rapsomanikis, S., Roberts, G., Schebeske, G., Sharma, S., Simo, R., Staubec, R., Turner, S., Uher, G. 1999. A global database of sea surface dimethylsulfide (DMS) measurements and a procedure to predict sea surface DMS as a function of latitude, longitude and month. *Global Biochemical Cycles* **13:** 399-444.

Knopf, D.A., and T. Koop (2006), Heterogeneous nucleation of ice on surrogates of mineral dust, *J. Geophys. Res.*, *111*, D12201.

Kong, F. et M. K. Yau. 1997. An Explicit Approach to Microphysics in MC2. *Atmosphere-Ocean,* **35**, 257-291.

Lohmann, U., Roeckner, E. 1996. Design and performance of a new cloud microphysics scheme developed for the ECHAM general circulation model. *Climate Dynamics* **12:** 557-572.

McFarlane, N.A., Boer, G.J., Blanchet J.-P., Lazare, M. 1992. The Canadian Climate Centre second-generation general circulation

model and its equilibrium climate. *Journal of Climate* **5:** 1013-1044.

Möhler, O., J. Schneider, S. Walter, A.J. Heymsfield, C. Schmitt, and Z.J. Ulanowski, How coating layers influence the deposition mode ice nucleation on mineral particles, in *International Conference on Clouds and Precipitation*, Cancun - Mexico, 2008.

Rinke, A., Dethloff, K. 2000. On the sensitivity of a regional Arctic climate model to initial and boundary conditions. *Climate Research* **14:** 101-113.

Salam, A., U. Lohmann, and G. Lesins (2007), Ice nucleation of ammonia gas exposed montmorillonite mineral dust particles, *Atmos. Chem. Phys.*, *7*, 3923–3931.

Schnell, R.C., 1984. Arctic haze and the Arctic Gas and Aerosol Sampling Program (AGASP). *Geophysical Research Letters* **11:** 361-364.

Shaw, G.E., 1995. The Arctic haze phenomenon. *Bulletin of the American Meteorological Society* **76:** 2403-2413.

K. Wyser, C. G. Jones, P. Du, E. Girard, U. Willén, J. Cassano, J. H. Christensen, J. A. Curry, K. Dethloff, J.-E. Haugen, D. Jacob, M. Køltzow, R. Laprise, A. Lynch, S. Pfeifer, A. Rinke, M. Serreze, M. J. Shaw, M. Tjernström and M. Zagar. 2008. An evaluation of Arctic cloud and radiation processes during the SHEBA year: simulation results from 8 Arctic regional climate models. *Climate Dynamics,*

Yli-Tuomi, T., Vanditte, L., Hopke, P.K., Shamasuzzoha Basunia, M., Landsberger, S., Viisanen, Y., Paatero, J. 2003. Composition of the Finnish Arctic aerosol: collection and analysis of historic filter samples. *Atmospheric Environment* **37:** 2355-2364